Hybrid Precoding for Millimeter Wave Cellular Systems with Partial Channel Knowledge

Ahmed Alkhateeb[†], Omar El Ayach[†], Geert Leus[‡], and Robert W. Heath Jr.[†]
[†] The University of Texas at Austin, Email: {aalkhateeb, oelayach, rheath},@utexas.edu
[‡] Delft University of Technology, Email: g.j.t.leus@tudelft.nl

***Abstract*—Next-generation cellular standards may leverage the large bandwidth available at millimeter wave (mmWave) frequencies to provide gigabit-per-second data rates in outdoor wireless systems. A main challenge in realizing mmWave cellular is achieving sufficient operating link margin, which is enabled via directional beamforming with large antenna arrays. Due to the high cost and power consumption of high-bandwidth mixed-signal devices, mmWave beamforming will likely include a combination of analog and digital processing. In this paper, we develop an iterative hybrid beamforming algorithm for the single user mmWave channel. The proposed algorithm accounts for the limitations of analog beamforming circuitry and assumes only partial channel knowledge at both the base and mobile stations. The precoding strategy exploits the sparse nature of the mmWave channel and uses a variant of matching pursuit to provide simple solutions to the hybrid beamforming problem. Simulation results show that the proposed algorithm can approach the rates achieved by unconstrained digital beamforming solutions.**

I. Introduction

Millimeter wave (mmWave) communication is one potential technology for future outdoor cellular systems [1]–[4]. Beamforming in outdoor mmWave systems will be critical in overcoming high pathloss and achieving reasonable link budgets. Large beamforming gains are made possible by the fact that, at mmWave frequencies, large antenna arrays can be packed into small form factors. Unfortunately, the high cost of mixed-signal components makes digital baseband beamforming, the default solution in microwave systems, impossible.

Analog RF beamforming solutions were proposed in [3], [5], [6], and were largely based on controlling the phase of the signal transmitted by each antenna via a network of analog phase shifters. Several solutions, known as beam training algorithms, were proposed to iteratively design the analog beamforming coefficients in systems without channel knowledge at the transmitter. In [5], a binary search beam training algorithm over a layered multi-resolution beamforming codebook was proposed, and a similar concept was used in the IEEE 802.15.3c standard [3]. In [6], multiple beams with unique signatures were simultaneously used to minimize the required beam training time. Unfortunately, the performance of analog strategies such as those in [3], [5], [6] is in general sub-optimal due to the limitations of by analog beamforming hardware. Such limitations are (i) the difficulty of controlling signal amplitude, and (ii) the potentially low-resolution signal phase control. To achieve larger beamforming gains, and to enable precoding multiple data streams, hybrid analog/digital processing strategies were proposed in [7]–[9]. In [7], an antenna selection-based algorithm was proposed to overcome the problem of having only a few RF chains to drive a larger number of transmit antennas; antenna selection, however, makes almost no use of the limited yet non-negligible digital capability of mmWave hardware. In [8], hybrid beamforming and combining algorithms were developed to minimize the received signal's mean-squared error in the presence of mmWave interference without actually attempting to maximize the mmWave link's spectral efficiency. In [9], the mmWave channel's sparse multipath structure [10]–[14], and the algorithmic concept of basis pursuit, were leveraged in the design of hybrid precoders that attempt approach capacity assuming perfect channel knowledge is available to the transmitter.

In this paper, we propose a single-user hybrid precoding algorithm for mmWave systems with large antenna arrays at both the base station (BS) and mobile station (MS). Motivated by the characteristics of mmWave propagation, we consider a propagation environment that is both reciprocal and sparse in multipath scattering [10]–[14]; channel reciprocity and sparsity are both exploited in precoder design. The proposed algorithm is designed to satisfy the constraints imposed by mmWave beamforming hardware such as (i) limited digital processing capability, (ii) constant gain constraints imposed by analog phase shifters, and (iii) the availability of only low-resolution quantized phase control. The proposed strategy relaxes the full channel knowledge assumption of [9] and assumes only partial knowledge at the BS and MS. Namely, each terminal is assumed to have knowledge of its *own local* angles of arrival (AoA) which can be obtained through spatial smoothing for example [15]. In the proposed strategy, precoders are designed in three stages. First, the BS exploits channel reciprocity and knowledge of its AoAs to transmit precoded pilot symbols that enable the MS to accurately estimate the gain on each propagation path. Based on the received pilots, the MS constructs an estimate of the channel's conditional covariance matrix by averaging over the unknown base station-side scattering. The MS then uses a variation of the matching pursuit algorithm from [9] to construct hybrid precoders that approximate the channel's dominant subspaces. The computation of precoders at the BS proceeds in a similar fashion. Simulations indicate that the spectral efficiency achieved by the proposed algorithm

The authors at The University of Texas at Austin were supported in part by Huawei Technologies and the Army Research Laboratory contract: W911NF-10-1-0420.

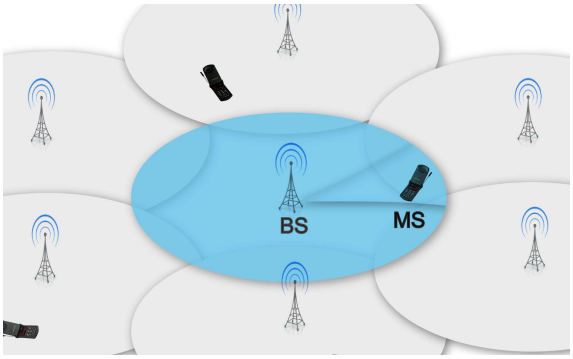

Fig. 1. A cell with a central basestation that uses directional transmission to serve one randomly located mobile user.

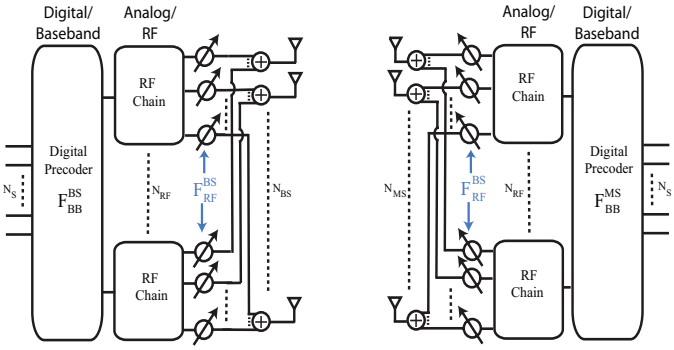

Fig. 2. Block diagram of BS-MS transceiver that uses RF and baseband beamformers at both ends

approach the rates achieved via optimal unconstrained digital precoding with full channel knowledge.

We use the following notation throughout this paper: $\mathbf{A}$ is a matrix, $\mathbf{a}$ is a vector, and a is a scalar, $\mathcal{A}$ is a set. $|\mathbf{A}|$ is the determinant of $\mathbf{A}$, $\|\mathbf{A}\|_F$ is its Frobenius norm, whereas $\mathbf{A}^T$, $\mathbf{A}^*$, $\mathbf{A}^{-1}$ are its transpose, conjugate transpose, and inverse respectively. $[\mathbf{A}]_{\mathcal{R},:}$ ($[\mathbf{A}]_{:,\mathcal{R}}$) are the rows (columns) of the matrix $\mathbf{A}$ with indeces in the set $\mathcal{R}$, and $\mathrm{diag}(\mathbf{a})$ is a diagonal matrix with the entries of $\mathbf{a}$ on its diagonal. $\mathbf{I}$ is the identity matrix and $\mathbf{1}_{N\times 1}$ is the N-dimensional all-ones vector. $\mathcal{N}(\mathbf{m},\mathbf{R})$ is a complex Gaussian random vector with mean $\mathbf{m}$ and covariance $\mathbf{R}$. $\mathbb{E}[\cdot]$ is used to denote expectation.

II. System Model

Consider the mmWave cellular system shown in Fig. 1. A BS with N_{BS} antennas and N_{RF} RF chains is assumed to communicate with a single randomly located MS with N_{MS} antennas and N_{RF} RF chains as shown in Fig. 2. The BS and MS communicate via N_{S} data streams, such that $N_{\mathrm{S}} \leq N_{\mathrm{RF}} \leq N_{\mathrm{BS}}$ and $N_{\mathrm{S}} \leq N_{\mathrm{RF}} \leq N_{\mathrm{MS}}$ [9], [16], [17].

On the downlink, the BS is assumed to apply an $N_{\mathrm{RF}} \times N_{\mathrm{S}}$ baseband precoder, $\mathbf{F}_{\mathrm{BB}}^{\mathrm{BS}}$, followed by an $N_{\mathrm{BS}} \times N_{\mathrm{RF}}$ RF precoder, $\mathbf{F}_{\mathrm{RF}}^{\mathrm{BS}}$. The sampled transmitted signal is therefore

$$\mathbf{x} = \mathbf{F}_{\mathrm{RF}}^{\mathrm{BS}}\mathbf{F}_{\mathrm{BB}}^{\mathrm{BS}}\mathbf{s}, \tag{1}$$

where $\mathbf{s}$ is the $N_{\mathrm{S}} \times 1$ vector of transmitted symbols, such that $\mathbb{E}[\mathbf{s}\mathbf{s}^*] = \frac{1}{N_{\mathrm{S}}}\mathbf{I}_{N_{\mathrm{S}}}$. Since $\mathbf{F}_{\mathrm{RF}}^{\mathrm{BS}}$ is implemented using analog phase shifters, its entries are constrained to satisfy $(\left[\mathbf{F}_{\mathrm{RF}}^{\mathrm{BS}}\right]_{:,i}\left[\mathbf{F}_{\mathrm{RF}}^{\mathrm{BS}}\right]_{:,i}^*)_{\ell,\ell} = N_{\mathrm{BS}}^{-1}$, where $(.)_{\ell,\ell}$ denotes the ℓ^{th} diagonal element, i.e., all entries are of equal norm. The total power constraint is enforced by letting $\|\mathbf{F}_{\mathrm{RF}}^{\mathrm{BS}}\mathbf{F}_{\mathrm{BB}}^{\mathrm{BS}}\|_F^2 = N_{\mathrm{S}}$.

We adopt a narrowband block-fading channel model in which an MS observes the received signal

$$\mathbf{r} = \sqrt{P}\mathbf{H}\mathbf{F}_{\mathrm{RF}}^{\mathrm{BS}}\mathbf{F}_{\mathrm{BB}}^{\mathrm{BS}}\mathbf{s} + \mathbf{n}, \tag{2}$$

where P is the average transmit power, $\mathbf{H}$ is the $N_{\mathrm{MS}} \times N_{\mathrm{BS}}$ matrix that represents the mmWave channel between the BS and MS, and $\mathbf{n} \sim \mathcal{N}(0,\sigma^2)$ is the Gaussian noise corrupting the received signal.

At the MS, the RF and baseband combiners $\mathbf{F}_{\mathrm{RF}}^{\mathrm{MS}}$ and $\mathbf{F}_{\mathrm{BB}}^{\mathrm{MS}}$ are used to process the received signal $\mathbf{r}$ which results in

$$\mathbf{y} = \sqrt{P}\mathbf{F}_{\mathrm{BB}}^{\mathrm{MS}*}\mathbf{F}_{\mathrm{RF}}^{\mathrm{MS}*}\mathbf{H}\mathbf{F}_{\mathrm{RF}}^{\mathrm{BS}}\mathbf{F}_{\mathrm{BB}}^{\mathrm{BS}}\mathbf{s} + \mathbf{F}_{\mathrm{BB}}^{\mathrm{MS}*}\mathbf{F}_{\mathrm{RF}}^{\mathrm{MS}*}\mathbf{n}. \tag{3}$$

The uplink signal model is identical to (3) with the roles of the precoders ($\mathbf{F}_{\mathrm{RF}}^{\mathrm{BS}}$, $\mathbf{F}_{\mathrm{BB}}^{\mathrm{BS}}$) and combiners ($\mathbf{F}_{\mathrm{RF}}^{\mathrm{MS}}$, $\mathbf{F}_{\mathrm{BB}}^{\mathrm{MS}}$) switched and with $\mathbf{H}$ replaced by $\mathbf{H}^T$ due to channel reciprocity.

Since mmWave channels are expected to have limited scattering [10]–[14], we adopt a geometric channel model with L scatterers. For simiplicity of exposition, we assume that $L \leq N_{\mathrm{RF}}$, though results can be generalized to the case of $N_{\mathrm{RF}} \leq L \leq \min(N_{\mathrm{BS}}, N_{\mathrm{MS}})$. Each scatterer is further assumed to contribute a single propagation path between BS and MS [9], [18]. Under this model, the channel $\mathbf{H}$ can be expressed as

$$\mathbf{H} = \sqrt{\frac{N_{\mathrm{BS}}N_{\mathrm{MS}}}{\rho L}}\sum_{\ell=1}^{L}\alpha_\ell \mathbf{a}_{\mathrm{MS}}\left(\phi_\ell^{\mathrm{MS}}\right)\mathbf{a}_{\mathrm{BS}}^*\left(\phi_\ell^{\mathrm{BS}}\right), \tag{4}$$

where α_ℓ is the complex gain of the ℓ^{th} path with $\mathbb{E}\left[|\alpha_\ell|^2\right] = 1$ and ρ is the pathloss between BS and MS. The variables $\phi_\ell^{\mathrm{BS}} \in [0, 2\pi]$ and $\phi_\ell^{\mathrm{MS}} \in [0, 2\pi]$ are the ℓ^{th} path's azimuth angles of departure or arrival respectively. Considering only the azimuth angles, and neglecting elevation, implies that the BS and MS implement horizontal (1-D) beamforming only. Extensions to 2-D beamforming are possible [9]. Finally, $\mathbf{a}_{\mathrm{BS}}\left(\phi_\ell^{\mathrm{BS}}\right)$ and $\mathbf{a}_{\mathrm{MS}}\left(\phi_\ell^{\mathrm{MS}}\right)$ are the antenna array response vectors at the BS and MS respectively. If uniform linear arrays (ULA) are assumed, $\mathbf{a}_{\mathrm{BS}}\left(\phi_\ell^{\mathrm{BS}}\right)$ can be written as

$$\mathbf{a}_{\mathrm{BS}}\left(\phi_\ell^{\mathrm{BS}}\right) = \frac{1}{\sqrt{N_{\mathrm{BS}}}}\left[1, e^{j\frac{2\pi}{\lambda}d\sin\left(\phi_\ell^{\mathrm{BS}}\right)}, \ldots \right. \\ \left. \ldots, e^{j(N_{\mathrm{BS}}-1)\frac{2\pi}{\lambda}d\sin\left(\phi_\ell^{\mathrm{BS}}\right)}\right]^T, \tag{5}$$

where λ is the signal wavelength, and d is the distance between antenna elements. The array response vectors at the MS, $\mathbf{a}_{\mathrm{MS}}\left(\phi_\ell^{\mathrm{MS}}\right)$, can be written in a similar fashion.

The channel in (4) can be given in a more compact form as

$$\mathbf{H} = \mathbf{A}_{\mathrm{MS}}\mathrm{diag}\left(\mathbf{z}\right)\mathbf{A}_{\mathrm{BS}}^* \tag{6}$$

where $\mathbf{z} = \sqrt{\frac{N_{\mathrm{BS}} N_{\mathrm{MS}}}{\rho L}} [\alpha_1, \alpha_2, ..., \alpha_L]^T$. The matrices

$$\mathbf{A}_{\mathrm{BS}} = \left[\mathbf{a}_{\mathrm{BS}}\left(\phi_1^{\mathrm{BS}}\right),\ \mathbf{a}_{\mathrm{BS}}\left(\phi_2^{\mathrm{BS}}\right),\ ...,\ \mathbf{a}_{\mathrm{BS}}\left(\phi_L^{\mathrm{BS}}\right)\right], \quad (7)$$

and

$$\mathbf{A}_{\mathrm{MS}} = \left[\mathbf{a}_{\mathrm{MS}}\left(\phi_1^{\mathrm{MS}}\right),\ \mathbf{a}_{\mathrm{MS}}\left(\phi_2^{\mathrm{MS}}\right),\ ...,\ \mathbf{a}_{\mathrm{MS}}\left(\phi_L^{\mathrm{MS}}\right)\right], \quad (8)$$

contain the BS and MS array response vectors respectively. Note, that by assumption, $\mathbf{A}_{\mathrm{BS}}$ is considered known to the BS, whereas $\mathbf{A}_{\mathrm{MS}}$ is considered known to the MS [15].

III. Hybrid Analog-Digital Beamforming Design

In this section we present a precoding algorithm for the system in Fig. 2 when both the BS and MS have knowledge of only their own set of local AoAs, i.e., the angles of incidence at the other terminal are unknown. The proposed algorithm leverages the structure of poorly scattering mmWave channels to provide near-optimal spectral efficiency using low complexity hardware.

We seek to design the hybrid precoders, ($\mathbf{F}_{\mathrm{RF}}^{\mathrm{BS}}$, $\mathbf{F}_{\mathrm{BB}}^{\mathrm{BS}}$, $\mathbf{F}_{\mathrm{RF}}^{\mathrm{MS}}$, $\mathbf{F}_{\mathrm{BB}}^{\mathrm{MS}}$), at both the BS and MS to maximize the mutual information achieved with Gaussian signaling over the mmWave link in (3) [19]. Regardless of whether uplink or downlink transmission is considered, the hybrid precoding problem can be summarized as directly maximizing the rate expression

$$R = \log_2 \left| I_{N_{\mathrm{S}}} + \frac{P}{N_{\mathrm{S}}} \mathbf{R}_{\mathrm{n}}^{-1} \mathbf{F}_{\mathrm{BB}}^{\mathrm{MS}*} \mathbf{F}_{\mathrm{RF}}^{\mathrm{MS}*} \mathbf{H} \mathbf{F}_{\mathrm{RF}}^{\mathrm{BS}} \mathbf{F}_{\mathrm{BB}}^{\mathrm{BS}} \times \mathbf{F}_{\mathrm{BB}}^{\mathrm{BS}\,*} \mathbf{F}_{\mathrm{RF}}^{\mathrm{BS}\,*} \mathbf{H}^* \mathbf{F}_{\mathrm{RF}}^{\mathrm{MS}} \mathbf{F}_{\mathrm{BB}}^{\mathrm{MS}} \right| \quad (9)$$

over the choice of feasible analog and digital processing matrices ($\mathbf{F}_{\mathrm{RF}}^{\mathrm{BS}}$, $\mathbf{F}_{\mathrm{BB}}^{\mathrm{BS}}$, $\mathbf{F}_{\mathrm{RF}}^{\mathrm{MS}}$, $\mathbf{F}_{\mathrm{BB}}^{\mathrm{MS}}$). Note that in (9), $\mathbf{R}_{\mathrm{n}}$ is the post-processing noise covariance matrix, i.e., $\mathbf{R}_{\mathrm{n}} = \mathbf{F}_{\mathrm{BB}}^{\mathrm{MS}*} \mathbf{F}_{\mathrm{RF}}^{\mathrm{MS}*} \mathbf{F}_{\mathrm{RF}}^{\mathrm{MS}} \mathbf{F}_{\mathrm{BB}}^{\mathrm{MS}}$ in downlink, and $\mathbf{R}_{\mathrm{n}} = \mathbf{F}_{\mathrm{BB}}^{\mathrm{BS}\,*} \mathbf{F}_{\mathrm{RF}}^{\mathrm{BS}\,*} \mathbf{F}_{\mathrm{RF}}^{\mathrm{BS}} \mathbf{F}_{\mathrm{BB}}^{\mathrm{BS}}$ in the uplink. For simplicity of exposition, we begin by summarizing the process with which the MS calculates the hybrid precoding matrices, ($\mathbf{F}_{\mathrm{RF}}^{\mathrm{MS}}$, $\mathbf{F}_{\mathrm{BB}}^{\mathrm{MS}}$), to be used on the uplink. Calculation of the downlink precoders used by the BS follows in an identical manner.

We propose to split the precoding problem into two stages. In the first stage, the BS transmits carefully constructed pilot symbols that allow the MS to estimate the complex gain on each of the channel's L propagation paths, *without knowledge of the BS-side angles of departure*. At the end of the channel training phase, the MS calculates the downlink channel's receive covariance matrix conditioned on its own angles of arrival and the newly estimated complex path gains. Since channels are assumed to be reciprocal, the *downlink's* conditional *receive* covariance matrix, calculated in the earlier stage, is itself the *uplink's* conditional *transmit* covariance and can thus be used for uplink precoder calculation. At this stage, the MS leverages the basis pursuit algorithm in [9] to compute $\mathbf{F}_{\mathrm{RF}}^{\mathrm{MS}}$ and $\mathbf{F}_{\mathrm{BB}}^{\mathrm{MS}}$ so that their combined effect, $\mathbf{F}_{\mathrm{RF}}^{\mathrm{MS}} \mathbf{F}_{\mathrm{BB}}^{\mathrm{MS}}$, approximates the dominant eigenvectors of the uplink's conditional transmit covariance.

In the remainder of this section, we formalize the proposed two-stage training/precoding strategy.

A. Downlink Channel Training:

Under the reciprocal channel assumption, the AoAs which are assumed to be known to the base station are themselves the AoDs for the BS-initiated transmissions. Since the BS-side AoDs are unknown to the MS, however, and in fact may be of little importance to the MS, the BS sends carefully precoded pilot symbols that allow the MS to estimate the complex gain on each of the channel's L propagation paths, *without knowledge of the BS-side angles of departure*. To achieve this, the BS precodes its pilots in a way that excites all paths uniformly. Equivalently, the BS finds training precoders that solve the under-determined equation

$$\mathbf{A}_{\mathrm{BS}}^* \left[\mathbf{F}_{\mathrm{RF}}^{\mathrm{BS}}\right]_{:,1:L} \left[\mathbf{F}_{\mathrm{BB}}^{\mathrm{BS}}\right]_{1:L,:} \mathbf{s}_{\mathrm{t}} = c\mathbf{1}_{1\times L}. \quad (10)$$

where $\mathbf{s}_{\mathrm{t}}$ is the vector of pilot symbols transmitted by the MS and c is a normalization constant that ensures power constraints are satisfied with equality. Note that we have explicitly given the subscripts $[\cdot]_{:,1:L}$ (where $1:L$ is used to denote the set of all integers from 1 to L) to highlight the fact that not all RF chains need to be used in this phase if $L < N_{\mathrm{RF}}$. Training precoders and pilots symbols can easily be found by setting $\mathbf{s}_{\mathrm{t}} = \mathbf{1}_{1\times L}$ and $\left[\mathbf{F}_{\mathrm{BB}}^{\mathrm{BS}}\right]_{1:L,:} = c(\mathbf{A}_{\mathrm{BS}}^* \left[\mathbf{F}_{\mathrm{RF}}^{\mathrm{BS}}\right]_{:,1:L})^{-1}$ for an arbitrary choice of $\mathbf{F}_{\mathrm{RF}}^{\mathrm{BS}}$. To ensure that the SNR in this estimation phase is sufficiently high, however, the columns of the constrained analog precoder $\left[\mathbf{F}_{\mathrm{RF}}^{\mathrm{BS}}\right]_{:,1:L}$ can be chosen to ensure that $\|\mathbf{A}_{\mathrm{BS}}^* \left[\mathbf{F}_{\mathrm{RF}}^{\mathrm{BS}}\right]_{:,1:L}\|_F$ is sufficiently large. This can be done via a simple search over a finite set of candidate analog beamformers for vectors with large projections on the columns of $\mathbf{A}_{\mathrm{BS}}$.

As a result of the precoded pilots, the received signal in the initial training phase can be written as

$$\mathbf{r} = \sqrt{\frac{P}{L}} \mathbf{H} \left[\mathbf{F}_{\mathrm{RF}}^{\mathrm{BS}}\right]_{:,1:L} \left[\mathbf{F}_{\mathrm{BB}}^{\mathrm{BS}}\right]_{1:L,:} \mathbf{s}_{\mathrm{t}} + \mathbf{n} \quad (11)$$

$$\stackrel{(a)}{=} \sqrt{\frac{P}{L}} \mathbf{A}_{\mathrm{MS}} \mathrm{diag}(\mathbf{z}) \mathbf{A}_{\mathrm{BS}}^* \left[\mathbf{F}_{\mathrm{RF}}^{\mathrm{BS}}\right]_{:,1:L} \left[\mathbf{F}_{\mathrm{BB}}^{\mathrm{BS}}\right]_{1:L,:} \mathbf{s}_{\mathrm{t}} + \mathbf{n} \quad (12)$$

$$\stackrel{(b)}{=} \sqrt{\frac{c^2 P}{L}} \mathbf{A}_{\mathrm{MS}} \mathbf{z} + \mathbf{n}, \quad (13)$$

where (a) is by recalling the channel model in (4) and (b) is due to the structure of precoded pilots in (10). Consequently, the scaled path gains $c\alpha_\ell$ can be estimated using a linear least squares estimator (LLSE)

$$\widehat{\mathbf{z}} = \sqrt{\frac{L}{P}} \left(\mathbf{A}_{\mathrm{MS}}^* \mathbf{A}_{\mathrm{MS}}\right)^{-1} \mathbf{A}_{\mathrm{MS}}^* \mathbf{r} \quad (14)$$

which can be implemented using the MS's hybrid analog/digital hardware by solving the equation $\left[\mathbf{F}_{\mathrm{BB}}^{\mathrm{MS}}\right]_{1:L,:}^* \left[\mathbf{F}_{\mathrm{RF}}^{\mathrm{MS}}\right]_{:,1:L}^* = \sqrt{\frac{L}{P}} \left(\mathbf{A}_{\mathrm{MS}}^* \mathbf{A}_{\mathrm{MS}}\right)^{-1} \mathbf{A}_{\mathrm{MS}}^*$. In systems where accurate phase control is possible, one can simply set $\mathbf{F}_{\mathrm{RF}}^{\mathrm{MS}} = \mathbf{A}_{\mathrm{MS}}$ and $\mathbf{F}_{\mathrm{BB}}^{\mathrm{MS}} = (\mathbf{A}_{\mathrm{MS}}^* \mathbf{A}_{\mathrm{MS}})^{-1}$). For cases with stricter constraints on analog circuitry, the same basis pursuit algorithm in [20] can be used approximate the LLSE in (14). More details on the basis pursuit framework are given in Section III-B.

Algorithm 1 Hybrid Analog-Digital Beamforming Design

$\mathcal{R} = \phi$
$\mathbf{F}_{\text{res}}$=$\mathbf{F}_{\text{opt}}^{\text{MS}}$
for $i \leq N_{\text{RF}}$ **do**
  $\mathbf{\Psi} = \mathbf{A}_{\text{can}}^{*}\mathbf{F}_{\text{res}}$
  $k = \arg\max_{j=1,2,..v_{\text{MS}}} \left(\mathbf{\Psi}^{H}\mathbf{\Psi}\right)_{j,j}$
  $\mathcal{R} = \mathcal{R} \cup k$
  $\mathbf{F}_{\text{RF}}^{\text{MS}} = [\mathbf{A}_{\text{can}}]_{:,\mathcal{R}}$
  $\mathbf{F}_{\text{BB}}^{\text{MS}} = \left(\mathbf{F}_{\text{RF}}^{\text{MS}*}\mathbf{F}_{\text{RF}}^{\text{MS}}\right)^{-1}\mathbf{F}_{\text{RF}}^{\text{MS}*}\mathbf{F}_{\text{opt}}^{\text{MS}}$
  $\mathbf{F}_{res} = \frac{\mathbf{F}_{\text{res}} - \mathbf{F}_{\text{RF}}^{\text{MS}}\mathbf{F}_{\text{BB}}^{\text{MS}}}{\|\mathbf{F}_{\text{res}} - \mathbf{F}_{\text{RF}}^{\text{MS}}\mathbf{F}_{\text{BB}}^{\text{MS}}\|_F}$
$\mathbf{F}_{\text{BB}}^{\text{MS}} = \sqrt{N_{\text{S}}}\frac{\mathbf{F}_{\text{BB}}^{\text{MS}}}{\|\mathbf{F}_{\text{RF}}^{\text{MS}}\mathbf{F}_{\text{BB}}^{\text{MS}}\|_F}$

B. Hybrid Uplink Precoder Design:

As a result of the downlink channel training phase, the MS now has knowledge of its own array response matrix $\mathbf{A}_{\text{MS}}$ and the estimated path gain vector $\widehat{\mathbf{z}}$. Thus, the MS may now calculate the downlink channel's scaled conditional receive covariance matrix

$$\mathbb{E}_{\mathbf{A}_{\text{BS}}|\mathbf{A}_{\text{MS}},\widehat{\mathbf{z}}}\left[\mathbf{H}\mathbf{H}^{*}\right] = \mathbf{A}_{\text{MS}}\text{diag}\left(\widehat{\mathbf{z}}\right)\text{diag}\left(\widehat{\mathbf{z}}\right)^{*}\mathbf{A}_{\text{MS}}^{*}. \quad (15)$$

where the subscripts in the expectation operator $\mathbb{E}_{\mathbf{A}_{\text{BS}}|\mathbf{A}_{\text{MS}},\widehat{\mathbf{z}}}[\cdot]$ indicate that expectation is taken over the distribution of $\mathbf{A}_{\text{BS}}$ and conditioned on the the MS's knowledge of $\mathbf{A}_{\text{MS}}$ and $\widehat{\mathbf{z}}$. Since, by reciprocity, the covariance matrix in (15) is itself the uplink *transmit covariance matrix*, the MS can now build its hybrid data precoders $\mathbf{F}_{\text{RF}}^{\text{MS}}$ and $\mathbf{F}_{\text{BB}}^{\text{MS}}$ to approximate the covariance's N_{S} dominant singular vectors denoted by the unconstrained precoder $\mathbf{F}_{\text{opt}}^{\text{MS}}$.

At this stage, we recall that the precoding capability of the system in Fig. 2 can be summarized as the ability to apply a set of N_{RF} constrained analog beamforming vectors, via the analog precoder $\mathbf{F}_{\text{RF}}^{\text{MS}}$, and form a linear combination of them via its digital precoder $\mathbf{F}_{\text{BB}}^{\text{MS}}$. Following the methodology in [9], and constraining the RF precoding columns to take values from a finite set of possible beamforming vectors, represented by the N_{can} columns of the candidate matrix $\mathbf{A}_{\text{can}}$, the problem of approximating the unconstrained precoder $\mathbf{F}_{\text{opt}}^{\text{MS}}$ can be written as [9]

$$\begin{aligned}(\mathbf{F}_{\text{RF}}^{\text{MS}\star}, \mathbf{F}_{\text{BB}}^{\text{MS}\star}) = \\ \arg\min \quad & \|\mathbf{F}_{\text{opt}}^{\text{MS}} - \mathbf{F}_{\text{RF}}^{\text{MS}}\mathbf{F}_{\text{BB}}^{\text{MS}}\|_F, \\ \text{s.t.} \quad & \left[\mathbf{F}_{\text{RF}}^{\text{MS}}\right]_{:,i} \in \left\{[\mathbf{A}_{\text{can}}]_{:,\ell} \mid 1 \leq \ell \leq N_{\text{can}}\right\}, \\ & \|\mathbf{F}_{\text{RF}}^{\text{MS}}\mathbf{F}_{\text{BB}}^{\text{MS}}\|_F^2 = N_{\text{S}}.\end{aligned} \quad (16)$$

The columns of the candidate matrix $\mathbf{A}_{\text{can}}$ can be chosen to satisfy arbitrary analog beamforming constraints. Two example candidate beamformer designs we consider in the simulations of Section IV are summarized as follows:

1) Equally spaced ULA beam steering vectors [20], i.e., a set of N vectors of the form $\mathbf{a}_{MS}(\frac{k\pi}{N})$ for $k = 0,\ 1,\ 2,\ \ldots, N-1$.

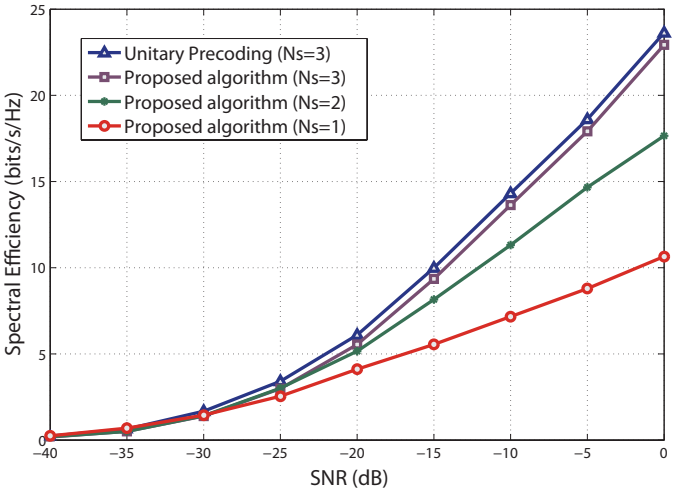

Fig. 3. Spectral efficiencies achieved by the proposed hybrid analog-digital precoding algorithm in a 200×100 mmWave system with 3 RF chains at both the BS and MS. The figure indicates that the proposed strategy can achieve near-optimal performance despite its low hardware complexity and reliance on partial channel knowledge.

2) Beamforming vectors whose elements can be represented as quantized phase shifts. In the case of quantized phase shifts, if each phase shifter is controlled by an N_{Q}-bit input, the entries of the candidate precoding matrix $\mathbf{A}_{\text{can}}$ can all be written as $e^{j\frac{k2\pi}{2^{N_{\text{Q}}}}}$ for some $k = 0,\ 1,\ 2,\ \ldots, 2^{N_{\text{Q}}} - 1$.

In summary, Algorithm 1 starts by finding the vector $[\mathbf{A}_{\text{can}}]_{:,\ell}$ along which $\mathbf{F}_{\text{opt}}^{\text{MS}}$, the precoder being approximated, has the maximum projection. It then appends the selected column vector $[\mathbf{A}_{\text{can}}]_{:,k}$ to the RF precoder $\mathbf{F}_{\text{RF}}^{\text{MS}}$. After the dominant vector is found and the least squares solution to $\mathbf{F}_{\text{BB}}^{\text{MS}}$ is calculated, the contribution of the selected vector is removed and the algorithm proceeds to find the column along which the "residual precoding matrix" $\mathbf{F}_{\text{res}}$ has the largest projection. The process continues until all N_{RF} beamforming vectors have been selected. At the end of the N_{RF} iterations, the algorithm would have: (i) constructed an $N_{\text{MS}} \times N_{\text{RF}}$ RF precoding matrix $\mathbf{F}_{\text{RF}}^{\text{MS}}$ and (ii) found the optimal $N_{\text{RF}} \times N_{\text{S}}$ baseband precoder $\mathbf{F}_{\text{BB}}^{\text{MS}}$ which minimizes the objective in (16).

C. Hybrid Downlink Precoder Design:

The calculation of hybrid downlink precoders proceeds identically to the uplink procedure. Namely, the MS transmits precoded pilots allowing the BS to estimate the downlink channel's conditional covariance matrix whose dominant eigenvectors are then approximated using Algorithm 1.

IV. Simulation Results

In this section, we present numerical results demonstrating the performance of the proposed algorithm in a single-cell mmWave cellular system. The simulated environment is assumed to have $L = 3$ scatterers with uniformly random angles of arrival and departure. The complex path gains are assumed to be Gaussian distributed with equal variances.

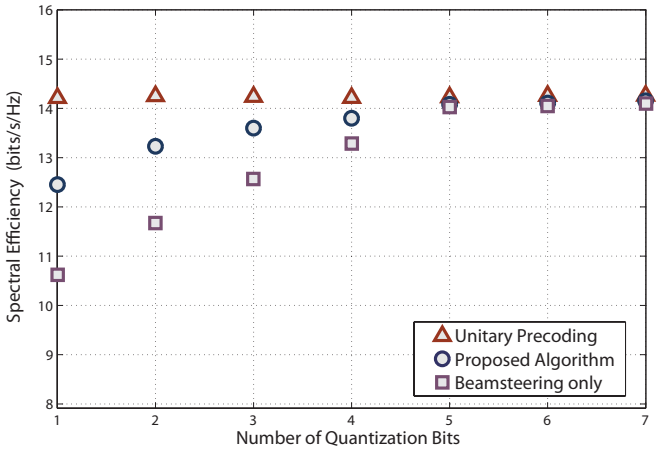

Fig. 4. Spectral efficiency as a function of phase quantization bits in a hybrid system with only quantized analog phase control. Results are reported for a 40×10 mmWave system at an SNR of 0dB.

The base station is assumed to have $N_{\mathrm{BS}} = 200$ antennas and the mobile station is assumed to have $N_{\mathrm{MS}} = 100$ antennas, you both have only $N_{\mathrm{RF}} = 3$ RF chains. The inter-element spacing in both BS and MS antenna arrays is set to half a wavelength. Fig. 3 plots the performance of the proposed precoding algorithm with a candidate RF $\mathbf{A}_{\mathrm{can}}$ precoding matrix consisting of 100 equally spaced ULA beam steering vectors. The performance of optimal unitary precoding for $N_{\mathrm{S}} = 3$ (which requires both perfect channel knowledge and unconstrained digital processing) is shown for comparison. Simulation results show that the proposed channel estimation and hybrid analog-digital precoding algorithm can achieve significant spectral efficiency via single or two-stream transmission and can achieve near-optimal data-rates for the case of three-stream transmission.

Fig. 4 investigates the negative effect of limiting analog phase control to a finite set of quantization levels. Namely, Fig. 4 plots the spectral efficiency achieved by the proposed algorithm as a function of the number of bits that control the phase shifters used in analog precoding. Fig. 4 indicates that only a few bits are needed to approach the performance of unconstrained precoding, and thus arbitrary phase control is unnecessary. Fig. 4 also compares the performance of the proposed hybrid precoding algorithm to a baseline beam steering solution that can be implemented solely in analog [20]. Fig. 4 indicates that there may be significant gains in spectral efficiency if both analog and digital precoding can be used.

V. Conclusion

In this paper we considered single user hybrid precoding in millimeter wave cellular systems. Using a realistic spatial channel model, we developed a simple precoding solution assuming only partial channel knowledge at the base station and mobile station in the form of AoA knowledge. The proposed algorithm finds an approximation to the dominant eigenvectors of the conditional channel covariance matrix observed by the BS and MS. The precoding strategy leverages channel sparsity, reciprocity, and the algorithmic concept of basis pursuit. We presented numerical results on the performance of the proposed algorithm and showed that it allows millimeter wave systems to approach their capacity limit.

References

[1] Z. Pi and F. Khan, "An introduction to millimeter-wave mobile broadband systems," *IEEE Communications Magazine*, vol. 49, no. 6, pp. 101–107, 2011.

[2] "IEEE 802.11ad standard draft D0.1." [Online]. Available: www.ieee802.org/11/Reports/tgad update.htm

[3] IEEE Standard 802.15.3c:, "Wireless medium access control (MAC) and physical layer (PHY) specifications for high rate wireless personal area networks (WPANs), amendement 2: Millimeter-wave-based alternative physical layer extension," October 2009.

[4] Standard ECMA-387, "High rate 60 GHz PHY, MAC and HDMI PAL." [Online]. Available: Available: http://www.ecma-international.org/

[5] J. Wang, Z. Lan, C. Pyo, T. Baykas, C. Sum, M. Rahman, J. Gao, R. Funada, F. Kojima, H. Harada *et al.*, "Beam codebook based beamforming protocol for multi-Gbps millimeter-wave WPAN systems," *IEEE Journal on Selected Areas in Communications*, vol. 27, no. 8, pp. 1390–1399, 2009.

[6] Y. Tsang, A. Poon, and S. Addepalli, "Coding the beams: Improving beamforming training in mmwave communication system," in *Proc. of IEEE Global Telecommunications Conference*, 2011, pp. 1–6.

[7] X. Zhang, A. Molisch, and S. Kung, "Variable-phase-shift-based RF-baseband codesign for MIMO antenna selection," *IEEE Transactions on Signal Processing*, vol. 53, no. 11, pp. 4091–4103, 2005.

[8] V. Venkateswaran and A. van der Veen, "Analog beamforming in MIMO communications with phase shift networks and online channel estimation," *IEEE Transactions on Signal Processing*, vol. 58, no. 8, pp. 4131–4143, 2010.

[9] O. El Ayach, R. W. Heath, Jr., S. Abu-Surra, S. Rajagopal, and Z. Pi, "Low complexity precoding for large millimeter wave MIMO systems," in *Proc. of IEEE International Conference on Communications*, June 2012, pp. 3724 –3729.

[10] P. Smulders and L. Correia, "Characterisation of propagation in 60 GHz radio channels," *Electronics & Communication Engineering Journal*, vol. 9, no. 2, pp. 73–80, 1997.

[11] H. Xu, V. Kukshya, and T. Rappaport, "Spatial and temporal characteristics of 60-GHz indoor channels," *IEEE Journal on Selected Areas in Communications*, vol. 20, no. 3, pp. 620–630, 2002.

[12] E. Ben-Dor, T. Rappaport, Y. Qiao, and S. Lauffenburger, "Millimeter-wave 60 GHz outdoor and vehicle AOA propagation measurements using a broadband channel sounder," in *IEEE Global Telecommunications Conference*, 2011, pp. 1–6.

[13] Q. Spencer, B. Jeffs, M. Jensen, and A. Swindlehurst, "Modeling the statistical time and angle of arrival characteristics of an indoor multipath channel," *IEEE Journal on Selected Areas in Communications*, vol. 18, no. 3, pp. 347–360, 2000.

[14] A. Sayeed and V. Raghavan, "Maximizing MIMO capacity in sparse multipath with reconfigurable antenna arrays," *IEEE Journal of Selected Topics in Signal Processing*, vol. 1, no. 1, pp. 156–166, 2007.

[15] S. Shakeri, D. Arianandа, and G. Leus, "Direction of arrival estimation using sparse ruler array design," *IEEE International Workshop on Signal Processing Advances in Wireless Communications*, pp. 525 –529, June 2012.

[16] P. Xia, S.-K. Yong, J. Oh, and C. Ngo, "A practical SDMA protocol for 60 GHz millimeter wave communications," *42nd Asilomar Conference on Signals, Systems and Computers*, pp. 2019 –2023, Oct. 2008.

[17] P. Xia, S. Yong, J. Oh, and C. Ngo, "Multi-stage iterative antenna training for millimeter wave communications," *in Proc. of IEEE Global Telecommunications Conference*, 2008.

[18] V. Raghavan and A. Sayeed, "Multi-antenna capacity of sparse multipath channels," *IEEE Transactions on Information Theory, under revision*, 2009.

[19] A. Goldsmith, S. Jafar, N. Jindal, and S. Vishwanath, "Capacity limits of MIMO channels," *IEEE Journal on Selected Areas in Communications*, vol. 21, no. 5, pp. 684–702, 2003.

[20] O. El Ayach, R. W. Heath, Jr., S. Abu-Surra, S. Rajagopal, and Z. Pi, "The capacity optimality of beam steering in large millimeter wave MIMO systems," in *Proc. of IEEE International Workshop on Signal Processing Advances in Wireless Communications*, June 2012, pp. 100 –104.